

EVALUATION OF THE R/C STRUCTURES SEISMIC RESPONSE BY MEANS OF NONLINEAR STATIC PUSH-OVER ANALYSES

GIUSEPPE FAELLA

Dipartimento di Analisi e Progettazione Strutturale, Università di Napoli Federico II, Italy

ABSTRACT

The prediction of the seismic behaviour of r/c framed structures by means of nonlinear static push-over analyses is compared with the results provided by nonlinear dynamic analyses. The comparison is carried out by examining the response of frames characterized by a different number of stories and designed according to the Eurocode 8 regulations for high ductility structures. The push-over analyses are conducted by assuming a nonlinear distribution of the lateral forces over the frame height, which are amplified until a target top displacement, computed by using a capacity spectrum method, is achieved. The dynamic analyses are performed by considering both simulated and natural earthquake records, typical of stiff soil conditions. The analyses carried out in the paper allow to identify the range of applicability within which the nonlinear static push-over analyses can give relevant information on displacements, structural damage and collapse mechanisms of the r/c building structures under earthquake excitations.

The results presented in this paper are based on work developed with the contribution of Prof. Andrei M. Reinhorn of the State University of New York at Buffalo, USA.

KEYWORDS

Push-over analyses, r/c frames, prediction of seismic behaviour, composite response spectra, damage indices.

INTRODUCTION

An accurate and realistic prediction of the seismic behaviour of reinforced concrete structures can be achieved by nonlinear dynamic analyses. However, despite the increasing efficiency of the available computational tools, at this time, the step-by-step nonlinear dynamic analysis is unfeasible in most practical applications. In fact, due to the need for implementing complex behavioural models, such analysis requires a significant computational effort, especially for large multistory buildings; furthermore, besides the dependence on the structure modeling, the results depend on the assumed input ground motion. For these reasons, all seismic codes allow to compute the pattern of internal actions, needed to determine the required strength of beams and columns, through elastic analyses. Nevertheless, more relevant information on the seismic behaviour of r/c structures can be gained by performing nonlinear static push-over analyses. In such analyses the structure is subjected to incremental lateral loads, characterized by a selected distribution over the height of the structure, and the response is computed as a selected deformation parameter, usually the top displacement, increases up to a target value, which should be close to the one expected under the design earthquake.

The nonlinear static push-over analyses are mainly a performance evaluation procedure which is usually not intended as an alternative direct method for designing the structural members but, rather, as a tool to obtain further insight into the seismic behaviour of structures (Krawinkler 1994). In fact, the push-over analyses can give information on the structural strength capacities and on the deformation demands as well as can identify discontinuity in the strength distribution and the regions potentially exposed to larger damage (Miranda and Bertero 1991, Lawson *et al.* 1994). In order to verify the range of applicability within which the information provided by such analyses can be considered satisfactory, a comparison with the results obtained through

step-by-step nonlinear dynamic analyses is carried out in this paper. The comparison is performed by varying two parameters which are believed to be more significant, such as the number of stories and the input ground motion. The frames have been designed according to the European seismic code provisions (Eurocode 8) for high ductility structures and the dynamic analyses have been performed by using several - natural and spectrum compatible generated - accelerograms which are representative of stiff soil conditions. The structural response has been evaluated in terms of interstory drifts and of structural damage; in particular, indices at story level and overall damage indices have been computed based on deformation and energy "consumption".

DESIGN OF FRAMES AND MODELING ASSUMPTIONS

Three-bay 3-, 6- and 9-story r/c symmetrical plane frames have been analysed in order to consider different realistic cases. All frames have bays 5000 mm wide and stories 3500 mm high and are subjected to gravity loads in addition to the seismic forces; in particular, a dead load D_L of 30 N/mm and a live load L_L of 15 N/mm have been considered. The design has been performed by using the Eurocode 2 and 8 provisions (CEC 1990, CEN 1994). Vertical and earthquake loads have been applied in a combination of $D_L+0.3L_L+E_L$; the earthquake load E_L has been computed by reducing the live loads through a coefficient equal to 0.15 for all stories except the top one, where it has been fixed equal to 0.30. Therefore, each frame has been designed for a seismic weight of 34.50 N/mm at the roof and of 32.25 N/mm at the other floors; however, at each level the relevant weight of beams and columns has been also considered. In order to design the member strengths, the internal forces in beams and columns due to the seismic loading have been computed by a modal response spectrum analysis. The soil profile A spectrum (stiff soil) has been used and a value of 0.40 g has been chosen for the design peak ground acceleration. Eurocode 8 rules for high ductility structures have been applied and a q -factor equal to 5 has been used to define the strength level of the frames. The column cross-section depth has been spliced by 50 mm every story; the beams have been constrained to be identical at each floor and the cross-section depth has been spliced by 100 mm every three stories. The cross-section capacities have been computed by considering a characteristic cylinder strength of 20 N/mm² for concrete and a characteristic yield strength of 440 N/mm² for steel. When designing the longitudinal and the shear reinforcement of beams and columns, the Eurocode 2 and 8 provisions concerning the minimum amount of reinforcement have been constantly taken into account. The beams and columns cross-section sizes are reported in Fig. 1, where the frame fundamental periods T_f , based on the member elastic properties, and the periods T_o , computed including the contribution of the reinforcement, are also indicated.

Both the nonlinear static push-over analyses and the step-by-step nonlinear dynamic analyses have been carried out by means of the IDARC 2D computer program (version 3.2) where a detailed modeling of the r/c members is implemented (Kunnath and Reinhorn 1994). In particular, a member by member macro-modeling is adopted for beams and columns and a distributed plasticity model is used to obtain the element stiffness matrix. The cyclic behaviour of the member cross-sections is modelled by a degrading moment-curvature relationship built on a non-symmetric trilinear envelope curve. The main points of such curve, corresponding to the cracking, the yielding and the ultimate bending moments, have been computed by adopting constitutive relationships which account for the confinement in the concrete and for the hardening in the steel; in such computation the characteristic strengths have been used for concrete and steel.

Regarding to the hysteretic properties to be defined when performing the dynamic analyses, the member cyclic behaviour has been represented with a hysteretic four parameter model (Kunnath and Reinhorn 1994); in particular, parameter α , which the stiffness degradation at unloading depends on, has been set equal to 2 while parameters β_d and β_e , which influence the ductility-based strength decay and the energy-controlled strength

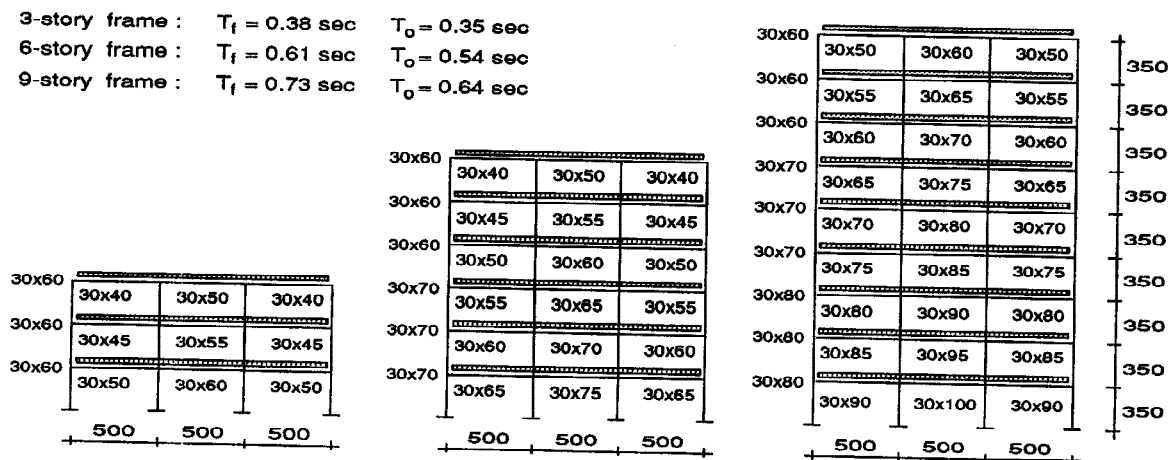


Fig. 1. Geometry of the examined frames.

Table 1. Input ground motions used in the study.

Earthquake	Date	Station	ID	Component	Duration [sec]	PGA [g]
Friuli	6.5.76	Tolmezzo	FT	EW	36.44	0.313
Montenegro	15.4.79	Petrovac	MP	NS	19.62	0.438
Montenegro	15.4.79	Hercegnovj	MH	EW	25.00	0.230
Parkfield	27.6.66	Parkfield	PK	N65E	43.78	0.495
Kern County	21.7.52	Taft	TF	S69E	54.40	0.179
Simulated accelerograms			A1+A5	-	25.00	0.40

deterioration, have been set equal to 0.10 and to 0.15 respectively; a value of 0.25 has been selected at the beam end sections and at the column-to-footing sections for the parameter γ , which controls the pinching, while a value of 0.30 has been selected at the other column end sections. The dynamic analyses have been performed assuming a Rayleigh damping of 5%.

In conclusion it has to be underlined that the adopted structure modeling yields a satisfactory simulation of the frame response if no significant deterioration of the joint properties is expected under the cyclic loading since joint behaviour is not explicitly represented by the computer model.

INPUT GROUND MOTIONS

Five simulated accelerograms and five historical earthquakes, which can be considered representative of stiff soil conditions, have been used in the dynamic analyses in order to be consistent with the adopted design spectrum. The characteristics of the selected records are reported in Table 1, but it has to be evidenced that in the analyses all records have been scaled at a peak ground acceleration of 0.4 g, which equals the design ground acceleration. The simulated accelerograms have been generated compatible with the elastic response spectrum defined by EC8 for stiff soils. The SIMQKE computer program (Gasparini 1976) has been used to generate the signals, by adopting an exponential intensity envelope function, a peak ground acceleration equal to 0.4 g and a duration of 25 seconds.

STATIC LATERAL LOAD PATTERN AND COLLAPSE MECHANISMS

It is well known that the nonlinear static push-over analyses involve applying a settled lateral load pattern and pushing the structures under these horizontal forces until a target deformation level is achieved. The lateral load pattern should be representative of the distribution of relative inertia forces which is acting on the structure during an earthquake. Obviously, relative values of forces should change as yielding spreads throughout the structural members and, then, the assumption of a constant lateral load pattern inevitably leads to an approximation. Nevertheless, constant load patterns are usually adopted and, frequently, the lateral load distribution is selected by referring to the inertia forces which activate in the elastic range of behaviour. In most cases a linear (inverted triangle) distribution, which is representative of the forces associated with the first vibration mode in low-rise regular buildings, is used. As the number of stories increases, the influence of higher modes of vibration is no longer negligible and the fundamental vibration mode lies approximately between a straight line and a parabola with a vertex at the base; therefore, a nonlinear shape of the lateral load pattern needs to be adopted for long period frames.

In this paper, the distribution of story forces has been defined as follows:

$$F_i = \frac{w_i h_i^k}{\sum_{j=1}^n w_j h_j^k} \cdot V_b \quad (1)$$

where w_i is the seismic weight of the i -th floor, h_i is the corresponding height from the base, n is the number of stories, V_b is the base shear and k is a coefficient which can be assumed to be dependent on the period T_o of the structure. The coefficient k can be settled equal to 1 for structures having period lower than 0.5 sec, thus leading to the inverted triangle distribution, and equal to 2 for $T_o > 2.5$ sec; a linear variation between 1 and 2 can be accepted to obtain a simple transition between the two extreme values (FEMA 1991). Based on values of periods T_o , the coefficient k has been set equal to 1.0, 1.06 and 1.1 for the 3-, 6- and 9-story frames respectively.

The obtained nondimensional base shear - top displacement curves are plotted in Fig.2: in particular, the base shear V_b has been nondimensionalized with respect to the frame seismic weight W , while the top displacement d_{top} is plotted as a percentage of the frame total height H . All curves are plotted up to a displacement corresponding to the first achievement of the ultimate curvature in a member cross-section. From Fig. 2 it can be seen that the

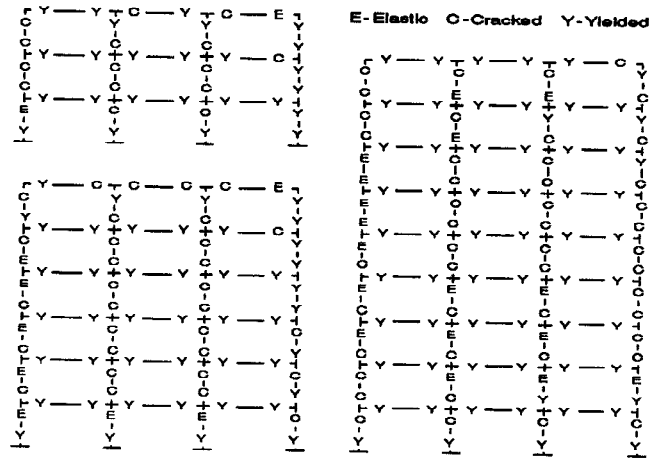
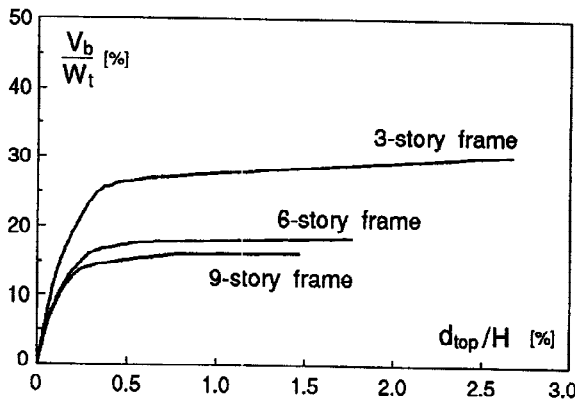


Fig. 2. Base shear - top displacement curves and static collapse mechanisms for the examined frames.

ultimate base shear coefficient V_b/W_t , for the 3-story frame is larger than the values obtained for the 6- and 9-story frames, which are similar. Besides the different overstrengths deriving from the design, such result is also due to the difference in the EC8 design spectrum values at the frame periods, which are equal to 0.20 g, 0.151 g and 0.134 g for the 3-, 6- and 9-story frame respectively: in fact, the variation in the base shear coefficients is rather proportional to the variation in the corresponding spectral values.

Figure 2 also presents the collapse mechanisms provided by the push-over analyses for the three examined frames. Such mechanisms are quite similar to those obtained through the nonlinear dynamic analyses by increasing the PGA (not shown for brevity): it follows that the push-over analyses can provide a good estimate of yielding distribution and of deformation demands in beams and columns and, therefore, they can clearly identify the critical member cross-sections. In the examined cases, it is particularly evident that EC8 provisions succeed to enforce the intended weak-beam strong-column dissipation mechanism: in fact, almost all of the beam end sections yield while most of the columns remain elastic or crack.

EVALUATION OF THE TOP DISPLACEMENT

The performance evaluation derived from the nonlinear static push-over analyses should be performed at a deformation level, usually controlled by the top displacement, similar to the one experienced by the structure under the considered earthquake. A faithful evaluation of such target top displacement can be obtained by using the capacity spectrum method (Freeman 1994): such procedure requires the computation of a spectrum representative of the inelastic strength and displacement demands and the computation of a capacity curve of the structure. If one considers MDOF systems, the demand curve may be represented by an elastic roof spectrum, computed for an equivalent viscous damping. Alternatively, for the sake of simplicity, the demand curve can be obtained by computing the elastic spectrum of a SDOF system and modifying the spectral values, in order to define an approximate inelastic spectrum. In both cases, the demand spectrum has to be represented in the Acceleration Displacement Response Spectrum (ADRS) format, that is by plotting the spectral accelerations S_a against the spectral displacements S_d with the frame fundamental period represented by radial lines. In fact, the intersection of such curve with the capacity curve, which can be identified with the base shear - top displacement curve, gives a prediction of the top displacement experienced by the structure under the selected earthquake. In this paper, the demand curve has been computed by using both the aforementioned procedures, in order to verify their reliability in the examined cases (r/c high ductility frames subjected to stiff soil earthquakes).

The composite highly damped spectra can be computed by assuming that the ratio of period T_j of the j -th vibration mode to the fundamental period T_0 is constant for any mode in respect to the first, independently of the value of T_0 . Under such hypothesis, the floor displacements d_i are given by (Reinhorn *et al.* 1995):

$$d_i(T, \nu) = \sqrt{\sum_{j=1}^N \left[\psi_{ij} g_j S_d \left(T, \nu, \frac{T_j}{T_0}, \frac{\nu_j}{\nu_0} \right) \right]^2} \quad (2)$$

while the base shear V_b is given by:

$$\frac{V_b}{W_t}(T, \nu) = \sqrt{\sum_{j=1}^N \left[g_j^2 S_a \left(T, \nu, \frac{T_j}{T_0}, \frac{\nu_j}{\nu_0} \right) \right]^2} \quad (3)$$

in which ψ_{ij} is the mass normalized modal shape j , g_j is the modal participation factor and ν_j is the damping

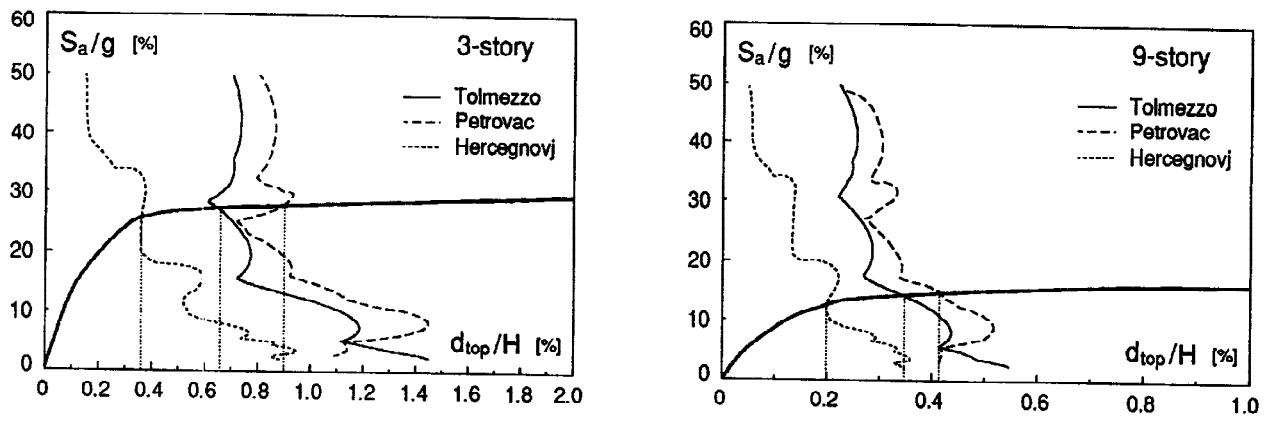


Fig. 3. Composite highly damped spectra vs capacity of frames.

ratio. In order to account for the hysteretic energy dissipation, it is possible to compute an equivalent viscous damping v_{eq} :

$$v_{eq} = v + \Delta v = v + \frac{4\gamma(\mu_{max} - 2)}{\pi\mu_{max}[2 + \alpha(\mu_{max} - 2)]} \quad (4)$$

which derives from an energy equivalence over a typical hysteretic loop (Reinhorn *et al.* 1995). In Equation (4), α and γ are coefficients which account for the pinching which characterizes the behaviour of r/c members, while μ_{max} is the maximum deformation ductility. With reference to this, it has to be evidenced that, particularly for highly inelastic structures, there are many uncertainties about the existence of a stable relationship between the hysteretic energy dissipation and the equivalent viscous damping, and especially about the values of parameters which have to be introduced. However, referring to Equation (4), if coefficients α and γ cover a range of values typical for r/c structures, it is easy to verify that the increment in damping Δv is slightly influenced by the variation in the coefficient α while Δv is more sensitive to the variation in γ ; furthermore, values of Δv are rather independent on the ductility for values of μ_{max} larger than about 5. In this paper, coefficients α and γ have been assumed equal to 0.05 and to 0.50 respectively, i.e. equal to the intermediate values among those recommended for r/c structures. Therefore, assuming $\mu_{max}=5$, Equation (4) gives a viscous equivalent damping v_{eq} equal to 0.23. Figure 3 shows, as an example, the evaluation of the top displacement for the 3- and the 9-story frames subjected to the Tolmezzo, Petrovac and Hercegnoj records.

By adopting the aforementioned second procedure, the inelastic spectra have been determined by a simple method derived from the one proposed by Vidic *et al.* (1994): in particular, the elastic spectral accelerations have been reduced by a coefficient k_a assumed to vary linearly between 1 and μ_d (being μ_d the ductility factor) in the short period region, while a constant reduction through $k_a=\mu_d$ has been considered in the medium and long period range, within which the equal-displacement principle is usually accepted; the displacements have been modified through the ratio μ_d/k_a . The transition period which separates the above two regions has been assumed equal to the predominant period of the input ground motion. The evaluation of the target top displacement by means of such procedure is shown in Fig. 4 for the same frames and records as those of Fig.3.

Table 2 presents the maximum top displacements obtained by means of dynamic inelastic analysis for the three examined frames subjected to the selected input ground motions, as well as the corresponding values computed by using the modal (MS) and the inelastic (IS) spectra; the displacements relative to the simulated accelerograms are the mean of the five computed values. Table 2 shows that, on the average, the estimate through the inelastic

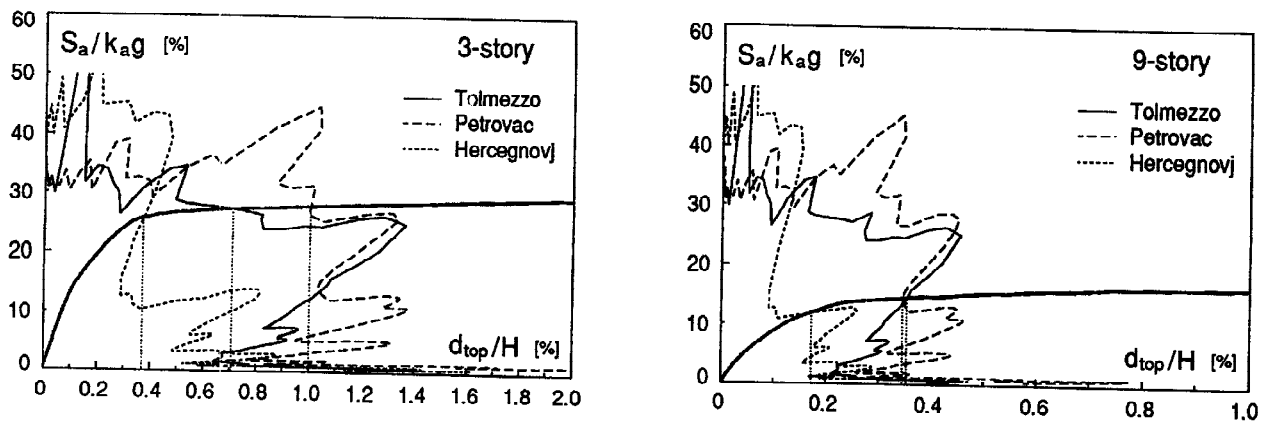


Fig. 4. Composite inelastic spectra vs capacity of frames.

Table 2. Dynamic, IS and MS predictions of the frame top displacement (in percent of H).

Earthquake	3-story frame			6-story frame			9-story frame		
	Dyn	MS	IS	Dyn	MS	IS	Dyn	MS	IS
Tolmezzo	0.71	0.66	0.72	0.52	0.56	0.54	0.35	0.35	0.36
Petrovac	1.01	0.90	1.00	0.53	0.50	0.54	0.35	0.41	0.34
Hercegnovj	0.39	0.36	0.38	0.27	0.30	0.25	0.21	0.20	0.18
Parkfield	0.88	0.95	0.94	0.75	0.90	0.65	0.66	0.80	0.50
Taft	0.61	0.78	0.70	0.55	0.70	0.45	0.42	0.60	0.38
Simulated	0.48	0.46	0.48	0.34	0.41	0.34	0.31	0.38	0.28

spectra is better than the one obtained by using the modal spectra; however, the error is nearly always lower than 10%, except for some values relative to the Parkfield and the Taft records.

EVALUATION OF DYNAMIC RESPONSE VERSUS PUSH-OVER RESULTS

As it has been evidenced in the introduction, the nonlinear static push-over analyses are mainly a tool which can be used to obtain further insight into the seismic behaviour of structures. In order to evaluate the ability of such analyses to give information on the structural damage, dynamic and static results in terms of interstory drifts and in terms of damage indices are compared in the following. Based on the results of the previous section, the response provided by the push-over analyses has been evaluated as top displacements equal to the ones predicted by using the composite inelastic spectra have been achieved.

Interstory drift

The interstory drift is a widely used parameter to get information on the seismic performance of multistory buildings: in fact, it can provide relevant information on deformation demand and, in many cases, it adequately reflects the potential structural or nonstructural damage. Since maximum interstory drifts at each level are experienced at different instants during the cyclic response, the maximum dynamic top displacement is smaller than the sum of the maximum dynamic interstory drifts. Therefore, if the top displacement is used to relate the results of the push-over analyses to the ones of the dynamic analyses, is advisable to compute the static interstory drifts for a maximum roof displacement higher than the dynamic one. Obviously, the increment in the target top displacement strongly depends on the characteristics of the input ground motion: moreover, an approximate evaluation can be performed independently of the seismic input but by increasing the target top displacement through a coefficient which increases with the number of stories.

In this paper, an increment of 10%, 20% and 30% has been adopted for the 3-, 6- and 9-story frames respectively and the results are reported in Fig. 5, where the maximum interstory drifts d/h obtained by the push-over and by the dynamic analyses are compared as the input ground motion varies. Figure 5 shows that values of d/h provided by the push-over analyses satisfactorily match the dynamic results, except for the 9-story frame subjected to the Parkfield and the Petrovac records. In the first case, the difference is due to the wrong prediction of d_{top} , while in the second case the maximum dynamic story drift is achieved at the top story because of the frequency content of the input and of the higher mode effects: in these conditions the push-over analysis is not able to predict the story deformations. However, based on the above results, it can be concluded that when the push-over analyses are used to evaluate the behaviour at the story level, the adoption of a target roof displacement larger than the dynamic one is really needed. The increment used herein in most cases leads to a satisfactory prediction of d/h , even if the estimate of d_{top} is not particularly adequate (see results obtained for the Taft record).

Damage index

The following modified version of the Park and Ang damage index (1985) has been used to determine damage at each member cross-section (Kunnath and Reinhorn 1994):

$$D = \frac{\theta_m - \theta_r}{\theta_u - \theta_r} + \frac{\beta_e E_h}{M_y \theta_u} \quad (5)$$

where θ_m is the maximum rotation attained during the load history, θ_u is the ultimate rotation capacity of the section, θ_r is the recoverable rotation at unloading, β_e is the strength degrading parameter, M_y is the yield moment of the cross-section, E_h is the dissipated hysteretic energy. Damage computed through the dynamic analyses is representative of damage at the achievement of the target top displacement; in the last case, the energy E_h has been computed as the area beneath the base shear - top displacement curve. The comparison between static and dynamic results has been carried out both at story level and at overall frame level: in order to compute the

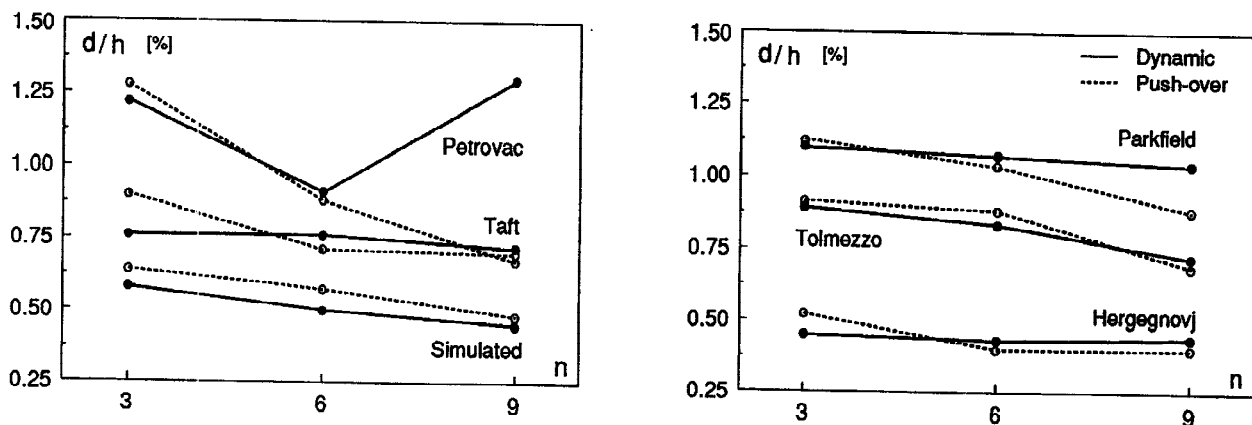


Fig. 5. Dynamic versus static interstory drift

corresponding indices, values of the index D obtained through Equation (5) have been combined using weighting factors based on the dissipated hysteretic energy at the component and at the story levels respectively.

Figure 6 displays damage in beams (D_b) and columns (D_c) at each story level for the examined frames subjected to the Tolmezzo record. It has to be evidenced that under such ground motion the procedure based on the use of the composite inelastic spectra provides values of the top displacements practically equal to the dynamic ones, but the results shown in Fig. 6 are representative also of those obtained by using the other selected input ground motions. Representation of Fig. 6 allows to easily identify the location and the severity of damage as well as to compare the results from the push-over analyses with those from the dynamic analyses. As it can be seen, the beams experience more damage than the columns, thus confirming the conclusion which has been drawn by examining the collapse mechanisms, that is the success of EC8 provisions to enforce the weak-beams strong-columns behaviour. The comparison between dynamic and static damage distribution, instead, shows that the push-over analyses well predict damage in the beams while underestimate damage in the columns: obviously, the excellent fitting of the beams damage is also due to the good prediction of the target top displacement. In any case, results of Fig. 6 confirm those obtained in terms of interstory drifts and, therefore, it seems advisable that also the prediction of damage in the columns through the push-over analyses is performed considering an increased target top displacement (larger than the dynamic one).

The comparison in terms of overall structural damage indices D_f is presented in Fig. 7 for all examined frames. In this case, values of damage indices provided by the push-over analyses have been computed for top displacements equal to those evaluated by the dynamic analyses, in order to verify the capacity of such analyses to predict the global damage, independently of errors in the top displacement evaluation. Values of D_f confirm that the push-over analyses are an efficient tool to predict the structural damage, notwithstanding a poor correlation has been found in terms of dissipated energy. In the examined cases, the maximum error in D_f is lower than 12% (except two cases) and it has to be underlined that such result has been obtained for frames

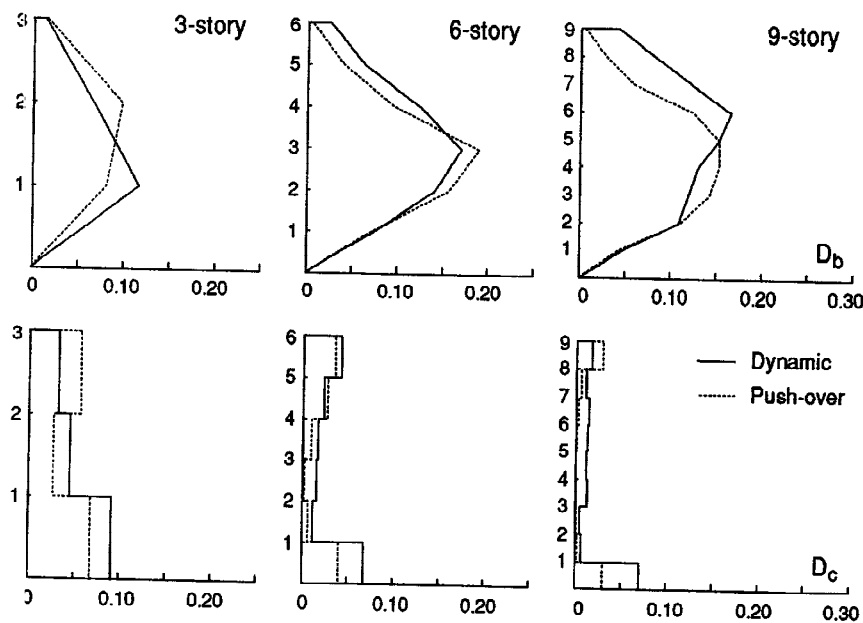


Fig. 6. Dynamic versus static damage distribution for beams (D_b) and columns (D_c).

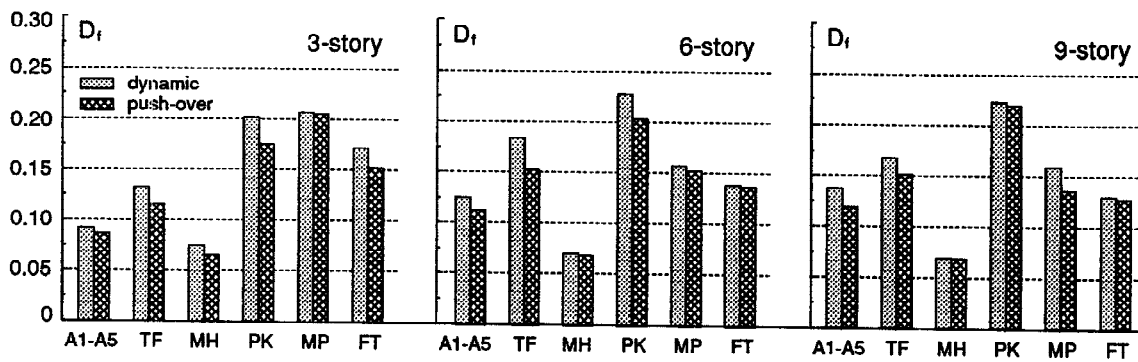


Fig. 7. Dynamic versus static overall structural damage index.

which experience different inelastic actions; in fact, D_f ranges between 0.07 and 0.23, being the value 0.40 considered as the threshold beyond which the structure is not repairable. Finally, it has to be evidenced that the good estimate obtained in the examined cases derives also from the use of input ground motions for which most of damage is due to the kinematic component.

CONCLUSION

The comparison of the response prediction obtained by means of nonlinear static push-over analyses with results from nonlinear dynamic time history analyses has allowed to show the capacity of the push-over analyses to assess the seismic response of r/c building structures, especially for the initial design steps. The analyses carried out in the paper have evidenced that such analyses can identify the collapse mechanisms and the critical regions, where larger deformations have to be expected, as well as may give relevant information on interstorey drifts and structural damage of r/c framed structures. It has been evidenced that the main issue is the prediction of the target top displacement up to which the response provided by the push-over analysis has to be evaluated; furthermore, it has been also shown that the interstorey drifts and the columns damage have to be computed at a top displacement larger than the maximum one expected under the considered earthquake. Based on the results shown in the paper, a prediction of the target displacement by using a capacity spectrum method seems to be a promising procedure, but further analyses need in order to have an efficient tool as the input ground motion characteristics vary. Finally, the suitability of the push-over analysis for structures subjected to input ground motions typical of soft soil conditions still need an assessment.

REFERENCES

- CEC (1990). *Eurocode 2 - Design of concrete structures - Part 1: General rules and rules for buildings*. Commission of the European Communities.
- CEN (1994). *Eurocode 8 - Design provisions for earthquake resistance of structures*. European Committee for Standardization, ENV 1998-1-1/2/3.
- FEMA (1991). *NEHRP Recommended Provisions for the Development of Seismic Regulations for New Buildings, Part 1: Provisions*. Federal Emergency Management Agency, Washington, D.C.
- Freeman S.A. (1994). The capacity spectrum method for determining the demand displacement. *ACI 1994 Spring Convention*, March.
- Gasparini D. (1976). SIMQKE: A program for artificial motion generation, user's manual and documentation. *Technical Report*, Dept. of Civil Engineering, M.I.T., Cambridge (Massachusetts).
- Krawinkler H. (1994). New trends in seismic design methodology. *10th European Conference on Earthquake Engineering*, Vienna, 821-830.
- Kunnath S.K. and A.M. Reinhorn (1994). IDARC 2D Version 3.2 - Inelastic damage analysis of RC building structures. *Users Manual*, State University of New York at Buffalo, September.
- Lawson R.S., V. Vance and H. Krawinkler (1994). Nonlinear static push-over analysis - why, when and how? *5th U.S. National Conference on Earthquake Engineering*, Chicago, 283-292.
- Miranda E. and V.V. Bertero (1991). Evaluation of seismic performance of a ten-story rc building during the Whittier Narrows earthquake. *Report No. UCB/EERC-91/10*, University of California, Berkeley.
- Park Y.J. and A.H. Ang (1985). Mechanistic seismic damage model for reinforced concrete. *J. of Structural Engineering*, **111**, No.4, 722-739.
- Reinhorn A.M., C. Li and M.C. Constantinou (1995). Experimental and analytical investigation of seismic retrofit of structures with supplemental damping - Part I: fluid viscous damping devices. *Technical Report NCEER-95-0001*, State University of New York at Buffalo.
- Vidic T., P. Fajfar and M. Fischinger (1994). Consistent inelastic design spectra: strength and displacement. *Earthquake Engineering and Structural Dynamics*, **23**, 507-521.